

Ethylene glycol-mediated direct synthesis of nanostructured nickel oxide–carbon composite material on nickel foam and its electrochemical property

Sa Lv, Chao Wang, Xiaotian Yang

Intelligent Building System Integration and Energy Control Laboratory, Jilin Institute of Architecture and Civil Engineering, Changchun 130118, People's Republic of China
E-mail: lvsa82@163.com

Published in *Micro & Nano Letters*; Received on 16th February 2013; Accepted on 13th March 2013

A convenient ethylene glycol (EG)-mediated one-pot solvothermal route was designed for direct synthesis of nanostructured nickel oxide–carbon composite material on nickel foam. EG was employed as solvent, complex agent and carbon source. Furthermore, cyclic voltammetry and constant current charge–discharge measurements confirmed that the composite material electrode displayed good electrochemical activity with a maximum specific capacitance of 539 F g^{-1} at a current density of 0.25 A g^{-1} .

1. Introduction: Considering the urgent demand for electrical energy storage, much effort has been focused on developing new electrode material and modifying the synthetic strategies that could provide desired control for the composition, structure and morphology of the active electrode material and optimise their properties thereby [1]. By far, significant advances have been achieved in the preparation of various types of electrode material [2]. Among them, transition metal oxides have been extensively investigated as alternative electrode materials owing to their high theoretical capacity based on a reversible faradic redox reaction. Especially, NiO has attracted considerable attention because of its low toxicity, natural abundance and high theoretical specific capacity [3–8]. However, the poor electrical conductivity of NiO limits its rate capability for high power performance, thus hindering its wide application in energy storage [9]. Consequently, binary composites have been constructed by loading and/or incorporating carbon materials to the metal oxide system. On the one hand, the metal oxide/carbon composites could improve electrical conductivity and mechanical strength and increase utilisation of active material [10]; on the other hand, they could enhance storage capacity owing to possible synergetic effects and other extended derived applications corresponding with different compositions [11]. For instance, metal oxide/carbon composites with different morphologies have been constructed by a variety of approaches, including electrospinning technique, electrochemical route and solvothermal synthesis etc. Among these composites, carbon sources were provided by glucose, polyacrylonitrile and block copolymer [12–16]. Furthermore, single-component materials could be obtained by postprocessing of the metal oxide/carbon composites. For example, metal oxide could be obtained by calcining the composite in oxygen atmosphere to remove carbon, and carbon nanostructures could be obtained by dissolving the composite with acid to remove metal oxide [17, 18].

Ethylene glycol (EG) is commonly used as a mediator of polyhydroxyl alcohol, especially, it was widely used as a solvent to synthesise metal oxides or metals owing to its strong reducing agent and high boiling point [19, 20]. According to the previous researches, synthesis of various metal oxides with different morphologies is possible by using a suitable metal salt in EG, where EG acted not only as a media, but also as the complex agent with metal ions for consequent polymerisation [10, 18]. Inspired by this idea, we here report a novel strategy for direct synthesis of NiO–C composite material on nickel foam through a mild one-pot solvothermal reaction of $\text{Ni}(\text{CH}_3\text{COO})_2$ and EG followed by a subsequent calcination process. Dehydration and carbonisation took place during heat

treatment under a highly pure nitrogen atmosphere. EG was exploited as a solvent, complex agent and carbon source. Moreover, such a direct growth with no complex assembly facilitates the electrochemical measurements and manipulation process [13, 21, 22].

2. Experimental section: All chemicals were of analytical grade and used without further purification. Nickel foam was washed with acetone, ethanol and deionised water several times before use. In a typical procedure, 4 g of $\text{Ni}(\text{CH}_3\text{COO})_2 \cdot 6\text{H}_2\text{O}$ was dissolved in 40 ml EG, and then the mixture and the pre-cleaned nickel foam were sealed into a 50 ml capacity Teflon-lined autoclave and heated at 160°C for 15 h. After cooling down to room temperature, nickel foam with green thin film on its surface was picked out and thoroughly rinsed with ethanol and deionised water. After that, subsequent calcination treatment was carried out at 450°C in a highly pure nitrogen atmosphere.

The structure and morphology of the product were characterised by a Rigaku X-ray diffractometer (XRD) with (Cu $K\alpha$ radiation $\lambda = 1.5406 \text{ \AA}$), scanning electron microscopy (FESEM, JEOL JSM-6700F, 5.0 kV) equipped with an energy dispersive X-ray spectrum (EDS). The electrochemical performance was evaluated on a CHI 660D model electrochemical workstation by cyclic voltammetry (CV) and a constant current discharge test by using a three-electrode cell with a pre-cleaned nickel foam as the counter electrode, Hg/HgO as the reference electrode, the obtained NiO–C composite material on nickel foam as the working electrode and 2 M KOH solution as electrolyte.

3. Results and discussion: Fig. 1*a* presents a typical SEM image of pristine nickel foam, showing its three-dimensional cross-linked porous structure, which can provide a high specific surface area for facilitating sufficient loading of active material [13]. An overview FESEM image of the products obtained through solvothermal reaction of $\text{Ni}(\text{CH}_3\text{COO})_2$ and EG and subsequent calcination process is shown in Fig. 2*b*, and uniform and dense products were observed on the nickel foam substrate. Figs. 2*c* and *d* are the magnified images, clearly showing that the products are roughwrought network structures composed of nanoparticles with diameters of 240–300 nm.

A corresponding XRD pattern is provided in Fig. 2*a*, and one can observe four peaks at 2θ of 37° , 43° , 63° and 75° corresponding to the (111), (200), (220) and (311) diffraction planes of the cubic structure of NiO (JCPDS Card No. 47-1049) in addition to the peaks marked with asterisks that are attributed to the nickel foam substrate (JCPDS 03-1051). Moreover, the pattern also confirms

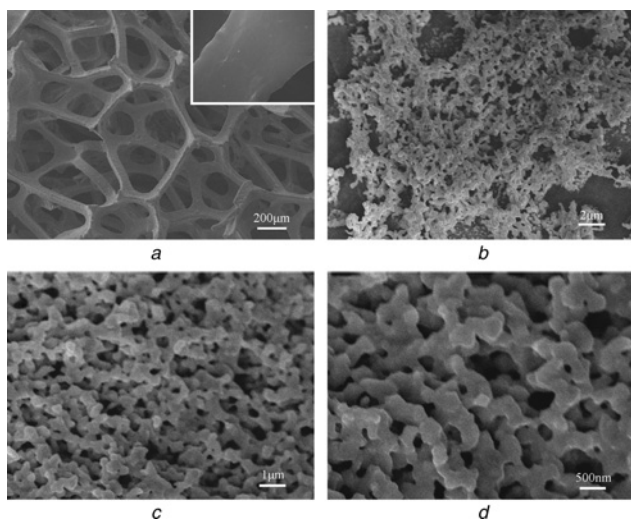


Figure 1 SEM images of samples
 a Pristine nickel foam
 b–d NiO–C composite material at different magnifications

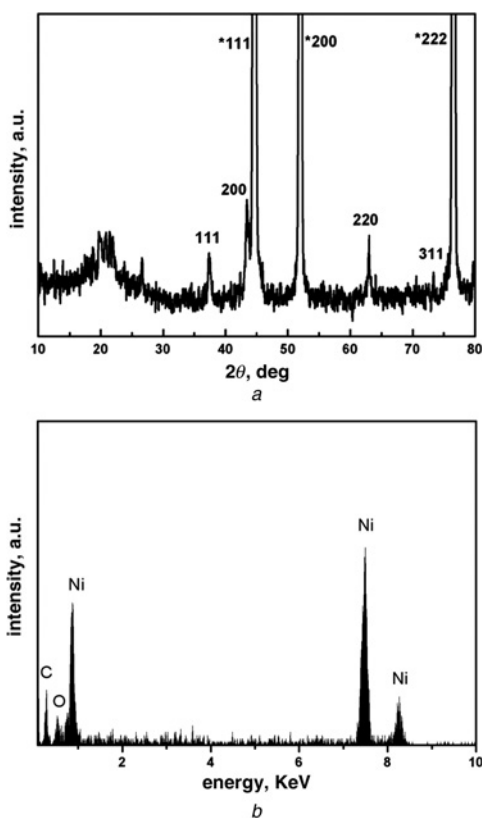


Figure 2 XRD and EDS pattern of NiO–C composite material
 a XRD pattern
 b EDS pattern

the existence of a broad diffraction peak centred at approximately $2\theta = 20^\circ$, which matches with the non-graphitic carbon [13]. The component of the composite material was characterised by EDS. Ni, O and C elements can be seen in Fig. 2b, showing that the products are mainly composed of NiO and C [17].

Based on the above results, we elucidate a plausible mechanism responsible for formation of NiO–C composite material. In our reaction system, EG performs three major roles in the growth of nickel oxide/carbon composite material. First, EG was used as a solvent. Secondly, when $\text{Ni}(\text{CH}_3\text{COO})_2 \cdot 6\text{H}_2\text{O}$ was mixed with

EG at 160°C , the $-\text{OCH}_2-\text{CH}_2\text{O}-$ chain was tightly bound with the nickel ions to produce nickel alkoxide, which precipitated to become the nuclei [23, 24], that is, EG acted as complex agent with nickel ions for polymerisation to form a polymeric network. Finally, subsequent calcination was carried out at 450°C in a highly pure nitrogen atmosphere, NiO–C composite is thus obtained and carbon source is provided by EG.

Typical CV curves of the NiO–C composite electrode and pristine nickel foam shown in Fig. 2a were measured in 2 M KOH solution and the potential ranges were 0–0.6 V (against Hg/HgO) at a scan rate of 10 mV/s. As shown in Fig. 2a, no well-defined peaks could be observed at the bare nickel foam. However, a couple of redox peaks are visible at the NiO–C composite electrode. This confirms that the electrochemical performance mainly originates from the NiO–C composite other than the nickel foam, and the redox reaction of NiO corresponds to the reaction: $\text{NiO} + \text{OH}^- \rightleftharpoons \text{NiOOH} + \text{e}^-$ [8]. Fig. 2b shows the CV curves of the NiO–C composite electrode in the potential range of 0–0.6 V (against Hg/HgO) at different scan rates. As the scan rate increases from 2 to 20 mV/s, the oxidation and reduction peaks potentials shift to more positive and negative positions, respectively, and the capacitance decreases inevitably. The decrease in capacitance may be explained by the fact that the inner active sites in the electrode are inaccessible at high scan rates because of ionic/electronic diffusion effect [6, 21]. The shapes of these CV curves do not significantly change, revealing the ideal capacitive behaviours of the composite electrode (Fig. 3).

The typical constant current charge–discharge tests were further carried out at various current densities of 0.25, 0.5, 0.75 and 1.0 A/g to evaluate the electrochemical properties and quantify specific capacitance of the NiO–C composite electrode (Fig. 4). As shown in Fig. 4a, the potential–time profiles exhibited symmetric charge–discharge features, indicating good capacitor behaviour and reversible redox reaction characteristics [6]. As the discharge current density decreases, the discharge curve displays a longer plateau (Fig. 4b).

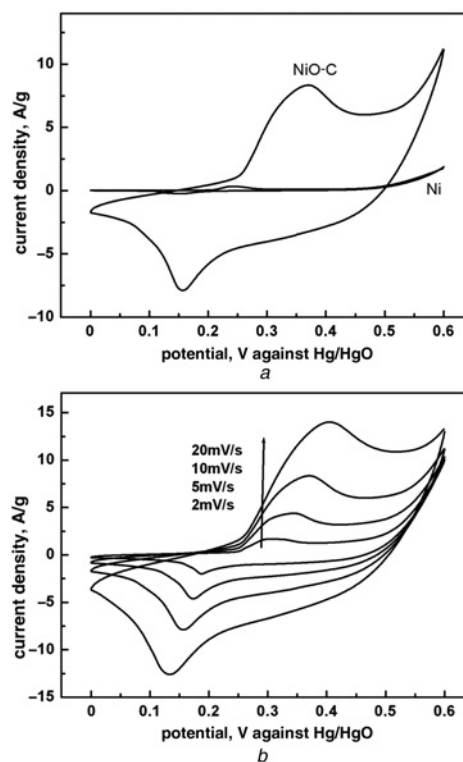


Figure 3 CV curves of composite electrode and pristine nickel foam; composite electrode at different scan rates

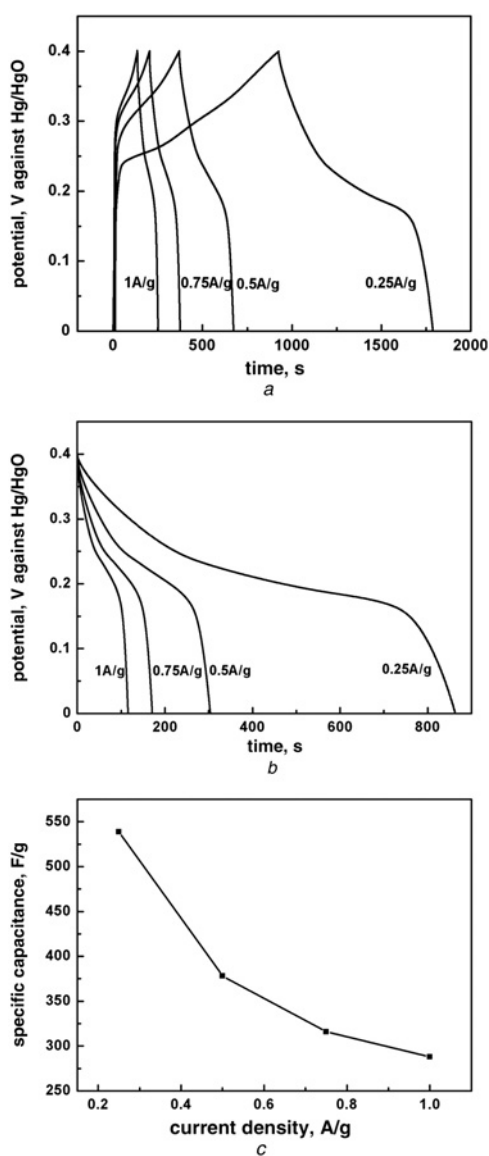


Figure 4 Charge–discharge curves (Fig. 4a) and discharge curves (Fig. 4b) of composite electrode at different discharge current densities; dependence of specific capacitance (Fig. 4c)

The specific capacitance decreases from 539 to 288 F/g as the discharge current density increases from 0.25 to 1 A/g. The specific capacitance was calculated according to the following formula

$$C_m = \frac{C}{m} = \frac{I \times \Delta t}{\Delta V \times m}$$

where C_m (F/g) is the specific capacitance, I (mA) is the charge–discharge current, Δt (s) is the discharging time, ΔV (V) represents the potential drop during discharge and m (mg) is the mass of the active material within the electrode. The dependence of specific capacitance on different current densities is shown in Fig. 4c. The longer the discharge time, the greater the corresponding specific capacitances. A possible reason is that the limited OH^- ions cannot intercalate swiftly at the electrode/electrolyte interface at higher current density [6]. Compared with our previously reported data of nickel oxide–carbon microspheres obtained by the hydrothermal method using glucose as carbon source [13], the specific capacitance of our current NiO–C composite on nickel foam is much higher. Such superior performances could be attributed to the composite using EG as carbon source with relatively small

size that provides a high specific surface area and shortens the electro diffusion pathway [25]. At the same time, specific capacitance obtained at smaller charge–discharge current densities is believed to be closer to that of the state with sufficient utilisation of the electrode material [26].

4. Conclusions: In conclusion, we have demonstrated a facile solvothermal strategy for one-pot synthesis of NiO–C composite electrode material on nickel foam, using EG as solvent, complex agent and carbon source. The composite material displayed good electrochemical activity with a maximum specific capacitance of 539 F/g at a current density of 0.25 A/g. The synthesis route presented here is robust and may be extended to fabricate other metal oxide/carbon composites for applications in electrochemical energy storage.

5. Acknowledgments: This work was supported by the National Natural Science Foundation of China (grant no. 51272089), and the 12th Five-Year Plan in Science and Technology of the Education Department of Jilin Province.

6 References

- [1] Ran L., Duay J., Lee S.B.: ‘Heterogeneous nanostructured electrode materials for electrochemical energy storage’, *Chem. Commun.*, 2011, **47**, pp. 1384–1404
- [2] Wang G.P., Zhang L., Zhang J.J.: ‘Review of electrode materials for electrochemical supercapacitors’, *Chem. Soc. Rev.*, 2012, **41**, pp. 797–828
- [3] Kim J.Y., Lee S.-H., Yan Y.F., *ET AL.*: ‘Controlled synthesis of aligned Ni–NiO core–shell nanowire arrays on glass substrates as a new supercapacitor electrode’, *RSC Adv.*, 2012, **2**, pp. 8281–8285
- [4] Cao C.Y., Guo W., Cui Z.M., *ET AL.*: ‘Microwave-assisted gas/liquid interfacial synthesis of flowerlike NiO hollow nanosphere precursors and their application as supercapacitor electrodes’, *J. Mater. Chem.*, 2011, **21**, pp. 3204–3209
- [5] Lu Q., Lattanzi M.W., Chen Y.P., *ET AL.*: ‘Supercapacitor electrodes with high-energy and power densities prepared from monolithic NiO/Ni nanocomposites’, *Angew. Chem. Int. Ed.*, 2011, **50**, pp. 6847–6850
- [6] Liang K., Tang X.Z., Hu W.C.: ‘High-performance three-dimensional nanoporous NiO film as a supercapacitor electrode’, *J. Mater. Chem.*, 2012, **22**, pp. 11062–11067
- [7] Zhu J.H., Jiang J., Liu J.P., *ET AL.*: ‘Direct synthesis of porous NiO nanowall arrays on conductive substrates for supercapacitor application’, *J. Solid State Chem.*, 2011, **184**, pp. 578–583
- [8] Li J.T., Zhao W., Huang F.Q., *ET AL.*: ‘Single-crystalline Ni(OH)₂ and NiO nanoplatelet arrays as supercapacitor electrodes’, *Nanoscale*, 2011, **3**, pp. 5103–5109
- [9] Li Q., Wang Z.L., Li G.R., *ET AL.*: ‘Design and synthesis of MnO₂/Mn/MnO₂ sandwich-structured nanotube arrays with high supercapacitive performance for electrochemical energy storage’, *Nano Lett.*, 2012, **12**, pp. 3803–3807
- [10] Wang H., Jiang P.L., Bo X.J., *ET AL.*: ‘Mesoporous carbon incorporated metal oxide nanomaterials as supercapacitor electrodes’, *Electrochim. Acta*, 2012, **65**, pp. 115–121
- [11] Li L., Wang T.T., Zhang L.Y., *ET AL.*: ‘Selected-control synthesis of monodisperse Fe₃O₄@C core-shell spheres, chains, and rings as high-performance anode materials for lithium-ion batteries’, *Chem. Eur. J.*, 2012, **18**, pp. 11417–11422
- [12] Mu J.B., Chen B., Guo Z.C., *ET AL.*: ‘Highly dispersed Fe₃O₄ nanosheets on one-dimensional carbon nanofibers: synthesis, formation mechanism, and electrochemical performance as supercapacitor electrode materials’, *Nanoscale*, 2011, **3**, pp. 5034–5040
- [13] Wang Y., Xing S.X., Zhang E.R., *ET AL.*: ‘One-pot synthesis of nickel oxide–carbon composite microspheres on nickel foam for supercapacitors’, *J. Mater. Sci.*, 2012, **47**, pp. 2182–2187
- [14] Sun B., Chen Z.X., Kim H.S., *ET AL.*: ‘MnO/C core-shell nanorods as high capacity anode materials for lithium-ion batteries’, *J. Power Sources*, 2011, **196**, pp. 3346–3349
- [15] Jiang H., Li C.Z., Sun T., *ET AL.*: ‘A green and high energy density asymmetric supercapacitor based on ultrathin MnO₂ nanostructures and functional mesoporous carbon nanotube electrodes’, *Nanoscale*, 2012, **4**, pp. 807–812

- [16] Lei Z.B., Shi F.H., Lu L.: 'Incorporation of MnO₂-coated carbon nanotubes between graphene sheets as supercapacitor electrode', *ACS Appl. Mater. Interfaces*, 2012, **4**, pp. 1058–1064
- [17] Fan L., Tang L., Gong H.F., *ET AL.*: 'Carbon-nanoparticles encapsulated in hollow nickel oxides for supercapacitor application', *J. Mater. Chem.*, 2012, **32**, pp. 16376–16381
- [18] Li W., Zhang F., Dou Y.Q., *ET AL.*: 'A self-template strategy for the synthesis of mesoporous carbon nanofibers as advanced supercapacitor electrodes', *Adv. Energy Mater.*, 2011, **1**, pp. 382–386
- [19] Xie X.W., Shang P.J., Liu Z.Q., *ET AL.*: 'Synthesis of nanorod-shaped cobalt hydroxycarbonate and oxide with the mediation of ethylene glycol', *J. Phys. Chem. C*, 2010, **114**, pp. 2116–2123
- [20] Wang S.Y., Jiang S.P., Wang X.: 'Microwave-assisted one-pot synthesis of metal/metal oxide nanoparticles on graphene and their electrochemical applications', *Electrochim. Acta*, 2011, **56**, pp. 3338–3344
- [21] Lv S., Suo H., Wang J.M., *ET AL.*: 'Facile synthesis of nanostructured Ni(OH)₂ on nickel foam and its electrochemical property', *Colloids Surf. A*, 2012, **396**, pp. 292–298
- [22] Wei J.T., Xing G.Z., Gao L., *ET AL.*: 'Nickel foam based polypyrrole–Ag composite film: a new route toward stable electrodes for supercapacitors', *New. J. Chem.*, 2013, **37**, pp. 337–341
- [23] Zhang G.H., Chen Y.J., Qu B.H., *ET AL.*: 'Synthesis of mesoporous NiO nanospheres as anode materials for lithium ion batteries', *Electrochim. Acta*, 2012, **80**, pp. 140–147
- [24] Xie X.W., Li Y., Liu Z.Q., *ET AL.*: 'Low-temperature oxidation of CO catalysed by Co₃O₄ nanorods', *Nature*, 2009, **458**, pp. 746–749
- [25] Liu D.Q., Wang Q., Qiao L., *ET AL.*: 'Preparation of nano-networks of MnO₂ shell/Ni current collector core for high-performance supercapacitor electrodes', *J. Mater. Chem.*, 2012, **22**, pp. 483–487
- [26] Lv S., Xing S.X.: 'Urea-induced direct synthesis of nanostructured α-Ni(OH)₂ on nickel foam', *Chem. Lett.*, 2011, **40**, pp. 1376–1377